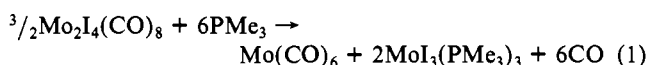
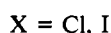
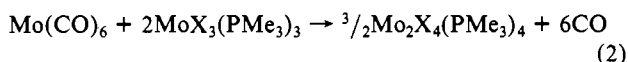


Once we had realized that the thermal interaction between $\text{Mo}_2\text{I}_4(\text{CO})_8$ and PMe_3 is a good synthetic method for compound **1**, we wondered if the same method could be applied to the preparation of the other halides. This indeed proved to be the case, as $\text{Mo}_2\text{Br}_4(\text{PMe}_3)_4$ (**2**), and $\text{Mo}_2\text{Cl}_4(\text{PMe}_3)_4$ (**3**) could be obtained in excellent yields from $\text{Mo}_2\text{X}_4(\text{CO})_8$ ($\text{X} = \text{Br}, \text{Cl}$) and PMe_3 with reaction conditions identical with those employed for the synthesis of compound **1**. Compounds **2** and **3** have been previously described.^{19,22,23} The spectroscopic properties of the $\text{Mo}_2\text{X}_4(\text{PMe}_3)_4$ ($\text{X} = \text{Cl}, \text{Br}, \text{I}$) series are reported in Table I. The ^1H NMR spectra present a broad peak with some emerging fine structure because of coupling to the ^{31}P nuclei system. The chemical shift moves downfield on going from chloride to iodide, which is opposite to what is expected from simple electronegativity considerations. This can possibly be attributed, according to a recent suggestion based on electrochemical work,²⁴ to an increased π -acceptor ability of the heavier halide. The ^{31}P NMR spectra show a singlet in the region between -9 and -15 ppm, which is quite typical for transition-metal-coordinated phosphines.²⁵

Comproportionation Reactions between $\text{MoX}_3(\text{PMe}_3)_3$ and $\text{Mo}(\text{CO})_6$. The identification of $\text{Mo}(\text{CO})_6$ among the disproportionation products of the $\text{Mo}_2\text{I}_4(\text{CO})_8$ - PMe_3 system made us consider the disproportionation stoichiometry represented in eq 1.



The identification of $\text{Mo}(\text{CO})_5(\text{PMe}_3)$ among the products could be ascribed to the presence of an excess of PMe_3 , although we cannot rule out that other $\text{Mo}(\text{III})$ products with a lower phosphine content are also formed during the disproportionation reaction. We were not able to isolate $\text{MoI}_3(\text{PMe}_3)_3$, nor other $\text{Mo}(\text{III})$ compounds, from the mixture arising from the interaction between $\text{Mo}_2\text{I}_4(\text{CO})_8$ and PMe_3 . If one considers, however, eq 1 to be a good approximation to the actual disproportionation process, one would expect the comproportionation of $\text{Mo}(\text{CO})_6$ and $\text{MoI}_3(\text{PMe}_3)_3$ in a 1:2 molar ratio to afford compound **1** when conditions are such that CO is forced out of the equilibrium (eq 2, $\text{X} = \text{I}$).



We actually find this to be the case, as refluxing $\text{Mo}(\text{CO})_6$ and $\text{MoI}_3(\text{PMe}_3)_3$ ¹⁵ (1:2 molar ratio) in toluene as solvent affords a solution containing no more carbonyl compounds, from which compound **1** could be isolated in about 55% yield. This reaction seems to take place about as fast as the synthesis of **1** from $\text{Mo}_2\text{I}_4(\text{CO})_8$ and PMe_3 . IR and UV/visible monitoring has also established the same behavior for the reaction between $\text{Mo}(\text{CO})_6$ and $\text{MoCl}_3(\text{PMe}_3)_3$, where compound **3** is formed (eq 2, $\text{X} = \text{Cl}$).

IR monitoring of these reactions shows the presence, after short reflux, of all of the known $\text{Mo}(\text{CO})_{6-n}(\text{PMe}_3)_n$ ($n = 0, 1, 2, 3$) compounds of molybdenum(0) (see Scheme I). Their formation as intermediates in this reaction seems perhaps too fast to be the result of CO substitution on $\text{Mo}(\text{CO})_6$ by free PMe_3 . Also, independent observations are not consistent with dissociation of the phosphine from $\text{MoI}_3(\text{PMe}_3)_3$ in refluxing toluene.¹⁵ A possible mechanism by which these intermediates could form involves oxidation of $\text{Mo}(\text{CO})_6$ to a 17-electron radical cation by the $\text{Mo}(\text{III})$ species. It is, in fact, well-known that CO substitutions on 18-e compounds are greatly accelerated by either chemical²⁶ or electrochemical²⁷ oxidation to 17-e intermediates.

The $\text{Mo}(\text{II})$ anion resulting from this electron-transfer reaction could then eliminate iodide and dimerize to the product while the 17-e $\text{Mo}(\text{I})$ cations could be neutralized by I^- , lose CO, and further react with $\text{Mo}(\text{III})$ to again produce the observed $\text{Mo}(\text{II})$ dimers.

Concluding Remarks

The molybdenum-iodide-phosphine-CO system appears to be a very complex one. Perhaps the most interesting result of this study is that our observations have allowed us to encompass in one scheme three of the different major areas of inorganic chemistry, i.e., carbonyl chemistry, classical Wernerian coordination chemistry, and the chemistry of multiple metal-metal bonds.

Evidence for disproportionation of PMe_3 -containing molybdenum(II) carbonyl complexes to $\text{Mo}(\text{0})$ and $\text{Mo}(\text{III})$ complexes has been found. This has led to the design of the comproportionation reaction between $\text{Mo}(\text{CO})_6$ and $\text{MoX}_3(\text{PMe}_3)_3$ that is also a new synthetic route to $\text{Mo}_2\text{X}_4(\text{PMe}_3)_4$ complexes.

We finally observe that the exploitation of the comproportionation reaction described in this paper should provide new synthetic routes to mixed-metal multiply bonded systems.

Acknowledgment. We thank Prof. D. J. Darensbourg for helpful discussion and the National Science Foundation for support of this work.

Registry No. **1**, 89637-15-0; **1-2THF**, 104010-56-2; **2**, 89707-70-0; **3**, 67619-17-4; $\text{Mo}_2\text{I}_4(\text{CO})_8$, 22547-54-2; $\text{Mo}_2\text{Br}_4(\text{CO})_8$, 80594-72-5; $\text{Mo}_2\text{Cl}_4(\text{CO})_8$, 104815-65-8; *mer*- $\text{MoI}_3(\text{PMe}_3)_3$, 107680-53-5; $\text{Mo}(\text{CO})_6$, 13939-06-5; Mo , 7439-98-7.

Supplementary Material Available: Full tables of bond distances, bond angles, and anisotropic displacement parameters for **1**-THF (3 pages); a listing of observed and calculated structure factors for **1**-THF (8 pages). Ordering information is given on any current masthead page.

- (26) (a) Bond, A. M.; Colton, R.; McCormick, M. J. *Inorg. Chem.* **1977**, *16*, 155. (b) Bond, A. M.; Grabaric, B. S.; Grabaric, Z. *Inorg. Chem.* **1978**, *17*, 1013. (c) Bond, A. M.; Colton, R.; McDonald, M. E. *Inorg. Chem.* **1978**, *17*, 2842. (d) Bly, R. S.; Silverman, G. R.; Hossain, M. M.; Bly, R. K. *Organometallics* **1984**, *3*, 642.
- (27) (a) Darchen, A.; Mahe, C.; Patin, H. *J. Chem. Soc., Chem. Commun.* **1982**, 243. (b) Jensen, S.; Robinson, B. H.; Simpson, J. J. *J. Chem. Soc., Chem. Commun.* **1983**, 1081. (c) Hershberger, J. W.; Klinger, R. J.; Kochi, J. K. *J. Am. Chem. Soc.* **1983**, *105*, 61. (d) Downard, A. J.; Robinson, B. H.; Simpson, J.; Bond, A. M. *J. Organomet. Chem.* **1987**, *320*, 363.

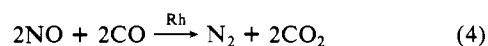
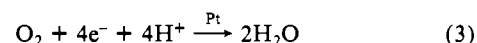
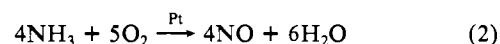
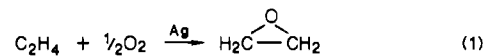
Contribution from the Department of Chemistry, University of Missouri—Columbia, Columbia, Missouri 65211

Late-Transition-Metal μ -Oxo and μ -Imido Complexes. 1. μ -Oxo Complexes of Rhodium and Iridium

Paul R. Sharp* and John R. Flynn

Received March 27, 1987

The chemical properties of oxygen atoms adsorbed on metal surfaces (oxygen adatoms) are important in many catalytic processes. Several metal-catalyzed reactions where adsorbed oxygen plays an important role are given below.¹⁻⁴



(23) Brown, P. R.; Cloke, F. G. N.; Green, M. L. H.; Tovey, R. C. *J. Chem. Soc., Chem. Commun.* **1982**, 519.

(24) Zietlow, T. C.; Hopkins, M. D.; Gray, H. B. *J. Am. Chem. Soc.* **1986**, *108*, 8266.

(25) Pregosin, P. S.; Kunz, R. W. ^{31}P and ^{13}C NMR of Transition Metal Phosphine Complexes; Diehl, P., Fluck, E., Kosfeld, R., Eds.; Springer-Verlag: New York, 1979.

(1) Grant, R. B.; Lambert, R. M. *J. Chem. Soc., Chem. Commun.* **1983**, 662-663 and references cited therein.

Our desire to model such surface species has led to our investigation of the synthesis and reactions of μ -oxo and isoelectronic μ -imido complexes of the late-transition metals Rh, Ir, Pd, Pt, and Au. Oxo⁵ and imido⁶ complexes of these metals are relatively rare and good synthetic methods for their preparations have yet to be developed. In addition, their chemical properties, especially those associated with the oxo and imido ligands, have not been extensively investigated.

In this paper we report the first preparations of Rh and Ir dpdm ($\text{dpdm} = \text{bis}(\text{diphenylphosphino})\text{methane}$) A-frame μ -oxo complexes. The oxo ligands in these complexes are unique in that they are highly basic, displaying reactivity patterns similar to those described for oxygen adatoms on late-transition-metal surfaces.⁷

Results

When $[\text{M}_2(\mu\text{-OH})(\text{CO})_2(\mu\text{-dpdm})_2]^+\text{X}^-$ ($\text{M} = \text{Rh}$, $\text{X} = \text{BF}_4$ or ClO_4 ; $\text{M} = \text{Ir}$, $\text{X} = \text{BF}_4$)^{8,9} in CH_2Cl_2 is treated with 1 equiv of $\text{LiN}(\text{SiMe}_3)_2$ the solution darkens slightly. The IR spectrum of the solution shows new carbonyl bands about 50 cm^{-1} lower than those of the starting hydroxo complexes. In vacuo removal of the CH_2Cl_2 leaves a solid that dissolves in aromatic hydrocarbon solvents. ³¹P NMR spectra show the presence of a single complex, and the ¹H NMR spectra have the expected phenyl resonances and a new methylene AB pair typical of dpdm A-frame complexes. The OH resonance is absent. If the solid is not completely dried, $\text{NH}(\text{SiMe}_3)_2$ can be detected.

All of the above observations are consistent with the deprotonation of $[\text{M}_2(\mu\text{-OH})(\text{CO})_2(\mu\text{-dpdm})_2]^+$ to give $\text{M}_2(\mu\text{-O})(\text{CO})_2(\mu\text{-dpdm})_2$. Nearly identical observations were made when $[\text{Rh}_2(\mu\text{-SH})(\text{CO})_2(\mu\text{-dpdm})_2]^+$ was deprotonated to give $\text{Rh}_2(\mu\text{-S})(\text{CO})_2(\mu\text{-dpdm})_2$.¹⁰ However, several other observations indicate that a modification of this formulation is required. A precipitate of LiX was not detected either in the reaction or in the workup (extraction into aromatic solvents). When petroleum ether is added to the toluene or CH_2Cl_2 solutions, a microcrystalline solid is obtained that shows bands in the mull IR spectra attributable to BF_4^- or ClO_4^- . Finally, when wet THF is added to the toluene solution ($\text{M} = \text{Rh}$, $\text{X} = \text{BF}_4$) a yellow precipitate forms, which IR and NMR data indicates is the BF_4^- salt of $[\text{Rh}_2(\mu\text{-OH})(\text{CO})_2(\mu\text{-dpdm})_2]^+$. On the basis of these observations the proper formulation of **1** must be $\text{M}_2(\mu\text{-O})(\text{CO})_2(\mu\text{-dpdm})_2\cdot\text{LiX}$

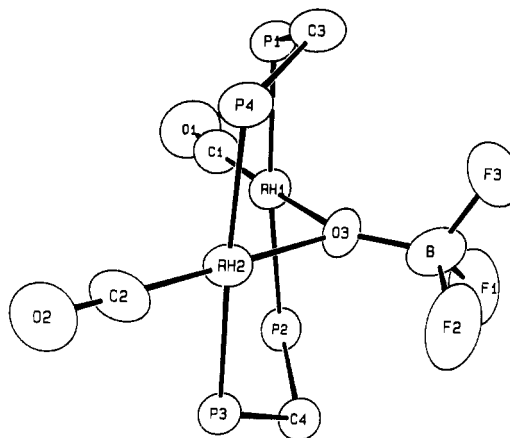


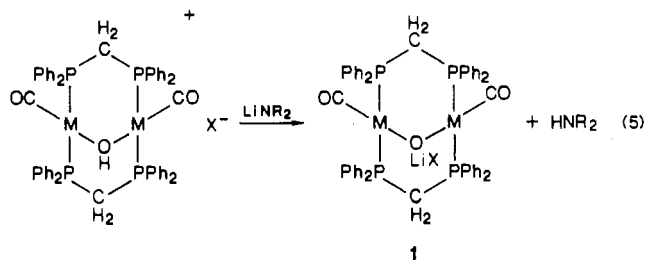
Figure 1. ORTEP drawing of $\text{Rh}_2(\mu\text{-OBF}_3)(\text{CO})_2(\mu\text{-dpdm})_2$ (**2**) (50% probability ellipsoids). Phenyl rings have been omitted for clarity.

Table I. Crystallographic and Data Collection Parameters for **2**

formula	$\text{C}_{52}\text{H}_{44}\text{BF}_3\text{O}_3\text{P}_4\text{Rh}_2 \cdot 1/2\text{CH}_2\text{Cl}_2$ (1156.91)
space group	$P2_1/c$
a , Å	17.901 (6)
b , Å	13.850 (5)
c , Å	21.304 (15)
β , deg	92.90 (4)
V , Å ³	5275.3
d_{calcd} , g/cm ³	1.46
Z	4
cryst size, mm	$0.2 \times 0.3 \times 0.3$
$\mu(\text{Mo K}\alpha)$, cm ⁻¹	8.35
transmissn range, %	99.7–100
scan width in θ , deg	$0.70 + 0.35 \tan \theta$
count stats, % (max time, s)	4 (60)
hkl range (2θ max, deg)	$-h, -k, \pm l$ (40.0)
no. of unique data (no. above 2σ)	4898 (3789)
no. of variables	608
$R(F_o)^a$	0.047
$R_w(F_o)^b$	0.068
error in observn of unit wt ^c	2.243
max shift/esd, final cycle	0.05

^a $R = \sum ||F_o| - |F_c|| / \sum |F_o|$. ^b $R_w = [\sum w(|F_o| - |F_c|)^2 / \sum wF_o^2]^{1/2}$; $w = 1/\sigma^2|F_o|$. ^c $[\sum w(|F_o| - |F_c|)^2 / (N_{\text{observns}} - N_{\text{params}})]^{1/2}$.

where the LiX interaction is via coordination of the μ -oxo group to the Li^+ (eq 5). The isolation of **1** is accompanied by partial

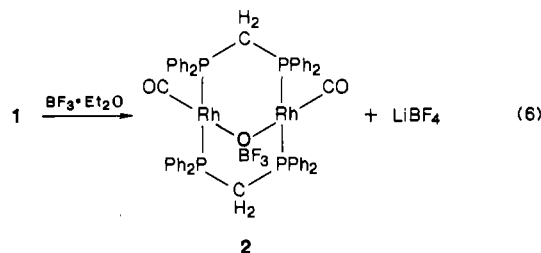


decomposition, and the solid never completely redissolves. Despite the decomposition, the solid analyses correctly for the above formulation.

The coordination of the oxo ligand to the Li^+ and the facile hydrolysis of **1** suggest an unusually basic oxo ligand. Consistent with this **1** ($\text{M} = \text{Rh}$, $\text{X} = \text{BF}_4$) reacts readily with $\text{BF}_3 \cdot \text{Et}_2\text{O}$ to give $\text{Rh}_2(\mu\text{-OBF}_3)(\text{CO})_2(\mu\text{-dpdm})_2$ (**2**) and a precipitate of LiBF_4 (eq 6). An analogous product, $\text{Ir}_2(\mu\text{-SBF}_3)(\text{CO})_2(\mu\text{-dpdm})_2$, was obtained when $\text{Ir}_2(\mu\text{-S})(\text{CO})_2(\mu\text{-dpdm})_2$ was treated with $\text{BF}_3 \cdot \text{Et}_2\text{O}$.¹¹ Stable crystals of **2** were obtained and subjected to an

- (2) Asscher, M.; Guthrie, W. L.; Lin, T.-H.; Somorjai, G. A. *J. Phys. Chem.* **1984**, *88*, 3233–3238.
- (3) Hoare, J. P. *The Electrochemistry of Oxygen*; Wiley-Interscience: New York, 1968; pp 143–151.
- (4) (a) Hecker, W. L.; Bell, A. T. *J. Catal.* **1979**, *59*, 223. (b) Loriner, P.; Bell, A. T. *J. Catal.* **1983**, *84*, 200.
- (5) (a) Nutton, A.; Bailey, P. M.; Maitlis, P. M. *J. Organomet. Chem.* **1981**, *213*, 313. (b) Brownlee, G. S.; Carty, P.; Cash, D. N.; Walker, A. *Inorg. Chem.* **1975**, *14*, 323–327. (c) Uemura, S.; Spener, A.; Wilkinson, G. *J. Chem. Soc., Dalton Trans.* **1973**, 2565. (d) Harrison, B.; Logan, N. *J. Chem. Soc., Dalton Trans.* **1972**, 1587. (e) de Boisbaudran, L. C. *R. Hebd. Seances Acad. Sci.* **1883**, *96*, 1336, 1404, 1551. (f) Cotton, F. A.; Lahuerta, P.; Sanan, M.; Schwotzer, W. *J. Am. Chem. Soc.* **1985**, *107*, 8282–8285. (g) Herrmann, W. A.; Bauer, C.; Plank, J.; Kalcher, W.; Speth, D.; Ziegler, M. L. *Angew. Chem., Int. Ed. Engl.* **1981**, *20*, 193–196. (h) Sumner, C. E., Jr.; Steinmetz, G. R. *J. Am. Chem. Soc.* **1985**, *107*, 6124. (i) Addison, A. W.; Gillard, R. D. *J. Chem. Soc. A* **1970**, 2523. (The complexes in this last article were reported as superoxo and peroxo complexes but were later found to be oxo complexes; as reported on p 52 in: Gubelmann, M. H.; Williams, A. F. *Struct. Bonding (Berlin)* **1983**, *55*, 1–65.) (j) Underhill, A. E.; Watkins, D. M. *J. Chem. Soc., Dalton Trans.* **1977**, 5. (k) Nesmeyanov, A. N.; Perevalova, E. G.; Struchkov, Yu. T.; Antipin, M. Yu.; Grandberg, K. I.; Dyadchenko, V. P. *J. Organomet. Chem.* **1980**, *201*, 343.
- (6) (a) Abel, E. W.; Blackmore, T.; Whitley, R. *J. Inorg. Nucl. Chem. Lett.* **1974**, *10*, 941–944. (b) McGlinchey, M. J.; Stone, F. G. A. *J. Chem. Soc., Chem. Commun.* **1985**, 868–869. (c) Muller, J.; Dorner, H.; Kohler, F. H. *Chem. Ber.* **1973**, *106*, 1122–1128.
- (7) (a) Madix, R. J.; Jorgensen, S. W. *Surf. Sci.* **1987**, *183*, 27–43. (b) Akhter, S.; White, J. M. *Surf. Sci.* **1986**, *167*, 101–126. (c) Berlowitz, P.; Yang, B. L.; Butt, J. B.; Kung, H. H. *Surf. Sci.* **1986**, *171*, 69–82. (d) Outka, D. A.; Madix, R. J. *J. Am. Chem. Soc.* **1987**, *109*, 1708–1714 and references cited therein.
- (8) Deraniyagala, S. P.; Grundy, K. R. *Inorg. Chem.* **1985**, *24*, 50–56.
- (9) Sutherland, B. R.; Cowie, M. *Organometallics* **1985**, *4*, 1637.
- (10) Kubiak, C. P.; Eisenberg, R. *Inorg. Chem.* **1980**, *19*, 2726–2732.

- (11) Kubiak, C. P.; Woodcock, C.; Eisenberg, R. *Inorg. Chem.* **1980**, *19*, 2733–2739.
- (12) Glowiak, T.; Kubiak, M.; Szymanska-Buzar, T. *Acta Crystallogr., Sect. B: Struct. Crystallogr. Cryst. Chem.* **1977**, *B33*, 1732–1737.



X-ray crystal structure analysis.

Structure of $\text{Rh}_2(\mu\text{-OBF}_3)(\text{CO})_2(\mu\text{-dppm})_2$ (2**).** An ORTEP drawing of the molecule, minus the phenyl groups, is shown in Figure 1. Selected bond distances and angles are given in Table III. The presence of the oxo bridge is confirmed as is the coordination of the oxo ligand to the BF_3 . The overall structure is typical of A-frame complexes and does not merit any comment except for the parameters related to the oxo ligand.

A comparison of the the oxo bond distances and angle of **2** with those of other structurally characterized Rh and Ir oxo complexes is given in Table IV. Among the Rh complexes the bonds in **2** are at the long end of the range whereas the angle is intermediate. The distances and angle are closest to those in $[\text{Rh}_3(\mu_3\text{-O})(\mu_2\text{-H})_3(\text{C}_5\text{Me}_5)_3]^+$ while the distances are considerably longer and the angle smaller than in $[\text{Rh}_3(\mu_3\text{-O})(\mu_2\text{-OAc})_6(\text{H}_2\text{O})_6]^+$. For the Ir complexes **2** is again at the long end of the range for the distances and intermediate for the angle. The most favorable comparison is with $\text{Ir}_2(\mu\text{-OH}\cdot\text{Cl})(\text{CO})_2(\mu\text{-dppm})_2$,⁹ the only other structurally characterized $\text{M}_2(\text{OX})$ A-frame complex, with essentially identical distances (2.06 (2) and 2.07 (2) Å) and angle (99.4 (8)°). The Rh–O distances in **2** also compare favorably, when corrected for the difference in covalent radii (0.29 Å), with the Rh–S distance of 2.367 (3) Å in $\text{Rh}_2(\mu\text{-S})(\text{CO})_2(\mu\text{-dppm})_2$.¹⁰ The Rh–S–Rh angle of 83.5 (1)° is somewhat smaller.

An unexpected feature of the structure is the coplanarity of the Rh, B, and oxo oxygen atoms. (The largest deviation from the least-squares plane is 0.05 Å.) We had expected an oxygen geometry consistent with sp^3 hybridization similar to that found in $\text{Ir}_2(\mu\text{-OH}\cdot\text{Cl})(\text{CO})_2(\mu\text{-dppm})_2$.⁹ The oxo oxygen planar geometry of **2** suggests sp^2 hybridization and oxygen lone pair occupation of a p orbital. This opens the possibility of oxygen p to Rh d π -donation. However, this does not seem probable given the low oxidation state of the Rh centers and their electron-rich nature. There is also no indication of multiple Rh–O bonding in the bond distances (see above), and the relatively high energy of the carbonyl bands in the IR spectrum of **2** is not consistent with π -donation. Another possible interaction is oxygen π -donation into B–F σ^* orbitals. The normal¹⁶ B–F bond distances do not seem to support such an interaction. Steric interactions combined with hydrogen bonding are apparently responsible for the oxygen planar geometry. F3 is directly in line with the methylene bridge carbon, C3, and their separation (3.169 (9) Å) is well within the sum of the van der Waals radii (3.50–3.60 Å). F1 and F2 straddle the other methylene bridge carbon, C4, with F1 within (3.236 (8) Å) and F2 at (3.523 (9) Å) the sum of the van der Waals radii. Additional close contacts of the fluorines with phenyl carbons (Table SVI)²³ also constrain the BF_3 group.

Discussion

Surfaces studies on late-transition metals indicate that the basicity of oxygen adatoms is a major factor in reactions of molecules on these metal surfaces.⁷ For Cu, Ag, and Au many molecules are unreactive in the absence of oxygen adatoms, and in their presence different reaction pathways may be followed depending on the acidity of the reacting molecule.^{7d} An important

Table II. Selected Positional Parameters for Complex **2**^a

atom	x	y	z	$B, \text{Å}^2$
Rh1	0.28946 (4)	0.14115 (6)	0.09805 (4)	2.98 (2)
Rh2	0.18889 (4)	0.31278 (6)	0.13566 (4)	3.08 (2)
P1	0.1807 (1)	0.0546 (2)	0.0737 (1)	3.27 (6)
P2	0.3963 (1)	0.2342 (2)	0.1124 (1)	3.02 (6)
P3	0.2979 (1)	0.3935 (2)	0.1635 (1)	2.83 (6)
P4	0.0828 (1)	0.2295 (2)	0.1024 (1)	3.34 (6)
F1	0.3088 (4)	0.2982 (6)	-0.0246 (3)	7.6 (2)
F2	0.2238 (5)	0.4040 (5)	0.0037 (3)	8.1 (2)
F3	0.1905 (4)	0.2671 (6)	-0.0463 (3)	8.1 (2)
B	0.2368 (6)	0.3043 (9)	-0.0003 (6)	3.8 (3)
O1	0.3658 (4)	-0.0348 (5)	0.1478 (4)	6.2 (2)
O2	0.1215 (4)	0.3855 (6)	0.2487 (4)	6.4 (2)
O3	0.2365 (3)	0.2602 (4)	0.0578 (3)	3.1 (1)
C1	0.3371 (5)	0.0335 (8)	0.1302 (5)	4.0 (2)
C2	0.1474 (5)	0.3571 (8)	0.2036 (5)	4.2 (3)
C3	0.1030 (5)	0.1340 (7)	0.0462 (5)	3.7 (2)
C4	0.3751 (5)	0.3642 (7)	0.1129 (4)	3.1 (2)

^a For the core atoms shown in Figure 1. Positional parameters for remaining atoms are given in Table IIS.²³ ^b Values for anisotropically refined atoms are given in the form of the isotropic equivalent displacement parameter defined as $4/3[a^2\beta(1,1) + b^2\beta(2,2) + c^2\beta(3,3) + ab(\cos \gamma)\beta(1,2) + ac(\cos \beta)\beta(1,3) + bc(\cos \alpha)\beta(2,3)]$.

Table III. Selected Bond Distances (Å) and Angles (deg) for **2**

Rh1–P1	2.324 (2)	Rh2–C2	1.769 (9)
Rh1–P2	2.315 (2)	F1–B	1.416 (9)
Rh1–O3	2.066 (4)	F2–B	1.40 (1)
Rh1–C1	1.833 (9)	F3–B	1.35 (1)
Rh2–P3	2.301 (2)	B–O3	1.38 (1)
Rh2–P4	2.304 (2)	O1–C1	1.131 (8)
Rh2–O3	2.037 (4)	O2–C2	1.157 (8)
P1–Rh1–P2	174.25 (7)	Rh1–O3–Rh2	98.6 (2)
R1–Rh1–O3	87.5 (1)	Rh1–O3–B	134.6 (4)
P1–Rh1–C1	91.9 (2)	Rh2–O3–B	126.4 (4)
P2–Rh1–O3	88.3 (1)	F1–B–F2	103.8 (7)
P2–Rh1–C1	92.2 (2)	F1–B–F3	104.4 (8)
O3–Rh1–C1	177.4 (3)	F1–B–O3	110.3 (6)
O3–Rh2–C2	179.3 (3)	F2–B–F3	108.7 (7)
P3–Rh2–P4	176.64 (8)	F2–B–O3	111.9 (7)
P3–Rh2–O3	90.0 (1)	F3–B–O3	116.7 (7)
P3–Rh2–C2	90.3 (2)	Rh1–C1–O1	177.2 (7)
P4–Rh2–O3	86.8 (1)	Rh2–C2–O2	178.8 (7)
P4–Rh2–C2	93.0 (2)		

Table IV. Oxo Bond Distances (Å) and Angles (deg)

compd	d(M–O)	M–O–M	ref
2	2.066 (4)	98.6 (2)	this work
	2.036 (4)		
	2.051 av		
$[\text{Rh}_3(\mu_3\text{-O})(\mu\text{-H})_3(\text{C}_5\text{Me}_5)_3]^+$	1.988 (6)	87.4 (2)	5a
	1.995 (6)	88.0 (2)	
	1.999 (6)	87.1 (2)	
	1.994 av	87.5 av	
$[\text{Rh}_3(\mu_3\text{-O})(\mu\text{-OAc})_6(\text{H}_2\text{O})_6]^+$	1.941 (12)	119.4 (6)	12
	1.906 (11)	120.1 (6)	
	1.924 (12)	120.5 (6)	
	1.93 (2)	118 (1)	
	1.94 (2)	120 (1)	
	1.90 (2)	121 (1)	
	1.92 av	120 av	
$\text{Ir}_2(\mu\text{-O})(\text{NO})_2(\text{PPh}_3)_2$	1.94 (1)	82.3 (3)	13
$\text{Ir}(\mu\text{-O})\text{Cl}_2(\text{NO})_2(\text{PPh}_3)_2$	1.897 (7)	134.4 (4)	14
	1.906 (8)		
	1.902 av		
$[\text{Ir}_2(\mu\text{-O})(\mu\text{-N}_2(o\text{-NO}_2\text{Ph}))(\text{NO})_2(\text{PPh}_3)_2]^+$	2.02 (4)	104 (2)	15
	1.85 (4)		
	1.94 av		

example of the latter case is the oxidation of alkenes on silver. Whereas ethylene can be selectively (ca 80%)¹⁷ oxidized to the epoxide (eq 1), propylene is mostly converted to CO_2 and H_2O .¹⁸

(13) Carty, P.; Walker, A.; Mathew, M.; Palenik, G. S. *J. Chem. Soc., Chem. Commun.* **1969**, 1374.

(14) Nyburg, S. C.; Cheng, P.-T. *Inorg. Chem.* **1975**, *14*, 327–329.

(15) Einstein, F. W. B.; Sutton, D.; Vogel, P. L. *Inorg. Nucl. Chem. Lett.* **1976**, *12*, 671–675.

(16) (a) Massey, A. G. *Adv. Inorg. Chem. Radiochem.* **1967**, *10*, 1–152. (b) Wells, A. F. *Structural Inorganic Chemistry*, 5th ed.; Oxford University Press: Oxford, England, 1984; p 1048.

(17) Kilty, P. A.; Sachtler, W. M. H. *Catal. Rev. Sci. Eng.* **1974**, *10*, 1–16.

Deprotonation of the relatively acidic methyl group of propylene by an oxygen adatom is believed to open a channel leading to complete combustion rather than epoxidation.¹⁹

The chemical properties of **1** clearly indicate the presence of a highly basic oxo ligand. The sulfido ligand in the Li free sulfur analogue of **1** is similarly basic but much less so. Theoretical²⁰ work on the sulfur complex indicates 45% sulfur character of the HOMO. For **1** the percent oxygen character of the HOMO must be even higher. High basicity is unique to **1** among the known oxo complexes of late-transition metals. (All other oxo complexes are stable in the presence of water, and most appear to be stable in at least weakly acidic media.) The reaction of **1** with water is particularly interesting in that it mimics the reaction of water with late-transition-metal oxygen adatoms (eq 7).^{7d,21} How



completely **1** will model late-transition-metal oxygen adatoms remains to be determined. We do not yet know if **1** is capable of oxidation reactions such as alkene epoxidation nor do we know if the oxo ligand is basic enough to deprotonate propylene. Future work will more thoroughly explore these aspects.

Experimental Section

General Procedures. All experiments were performed under a dinitrogen atmosphere in a VAC drybox or by Schlenk techniques. Solvents were carefully dried under dinitrogen by recommended published techniques.²² Petroleum ether with a boiling range of 35–60 °C was used. $[\text{M}_2(\mu\text{-OH})(\text{CO})_2(\mu\text{-dppm})_2]^+$ salts were prepared according to literature procedures.^{8,9} The Rh complexes must be recrystallized from CH_2Cl_2 /ether to remove traces of water. Solid $\text{Li}[\text{N}(\text{SiMe}_3)_2]$ was obtained by reducing and cooling hexane solutions from Aldrich. $\text{BF}_3\cdot\text{Et}_2\text{O}$ was used as received (Aldrich). NMR shifts are reported in ppm referenced to TMS for ¹H and ¹³C, and to external H_3PO_4 for ³¹P. Microanalyses were preformed (drybox) by Gailbrath microanalytical labs.

Preparation of $\text{M}(\mu\text{-O})(\text{CO})_2(\mu\text{-dppm})_2\text{-LiX}$ (1**: $\text{M} = \text{Rh}$, $\text{X} = \text{BF}_4$ or ClO_4 ; $\text{M} = \text{Ir}$, $\text{X} = \text{BF}_4$).** The following procedure for $\text{M} = \text{Rh}$ and $\text{X} = \text{BF}_4$ is typical. $\text{LiN}(\text{SiMe}_3)_2$ (18 mg, 0.10 mmol) in 1 mL of petroleum ether was added with stirring to a cold (ca 0 °C) solution of $[\text{Rh}(\mu\text{-OH})(\text{CO})_2(\mu\text{-dppm})_2]^+\text{BF}_4^-$ (103 mg, 0.100 mmol) in 5 mL of CH_2Cl_2 . An additional 10 mL of petroleum ether was added, and the solution was filtered. After the addition of another 5 mL of petroleum ether, the cloudy solution was cooled to –40 °C for 1 h. The resulting yellow crystal clusters (72 mg, 69%) were isolated by decantation (washed with petroleum ether and dried in vacuo).

Data for $\text{M} = \text{Rh}$, $\text{X} = \text{BF}_4$. Anal. Calcd (found) for $\text{C}_{52}\text{H}_{44}\text{BF}_4\text{LiO}_3\text{P}_4\text{Rh}_2$: C, 54.76 (54.52); H, 3.90 (3.90). IR (CH_2Cl_2 ,

cm^{-1}): 1941 s, 1929 vs. IR (mineral oil mull, cm^{-1}): 1930 s, 1918 vs, 1050 s. If solid **1** is isolated from toluene the mineral oil mull has ν_{CO} at 1937 s and 1926 vs cm^{-1} . ³¹P NMR (C_6D_6 , 121 MHz, 15 °C): 21.2 (d, $J_{\text{RHP}} = 139$ Hz). ¹H NMR (C_6D_6): 6.87–7.90 (m, phenyl), 4.92 and 2.68 (m, CH_2). Data for the ClO_4 salt were essentially the same.

Data for $\text{M} = \text{Ir}$, $\text{X} = \text{BF}_4$ (orange solid). IR (mineral oil mull, cm^{-1}): 1928 sh, 1914 vs. ³¹P NMR ($\text{THF}/\text{C}_6\text{D}_6$, 121 MHz, 15 °C): 12.6.

Preparation of $\text{Rh}(\mu\text{-OBF}_3)(\text{CO})_2(\mu\text{-dppm})_2$ (2**).** A solution of **1** in 3 mL of CH_2Cl_2 was prepared as described above starting with 21 mg (0.02 mmol) of $[\text{Rh}(\mu\text{-OH})(\text{CO})_2(\mu\text{-dppm})_2]^+\text{BF}_4^-$. All volatiles were removed in vacuo, and the residue was redissolved in 3 mL of CH_2Cl_2 . $\text{BF}_3\cdot\text{Et}_2\text{O}$ (3 μL , 0.02 mmol) was added with stirring. The solution was filtered to remove LiBF_4 , petroleum ether (10 mL) was added, and the mixture was cooled to –40 °C for 12 h. The resulting yellow solid was removed by filtration, washed with petroleum ether, and dried in vacuo. Yield: 15 mg (71% based on 0.5 CH_2Cl_2 of crystallization).

¹H NMR (90 MHz, CDCl_3): 7.20–7.80 (m, phenyl), 5.32 (s, CH_2Cl_2), 4.15 and 3.70 (m, CH_2). ³¹P NMR (121 MHz): 20.0 ($J_{\text{RHP}} = 113.2$ Hz). IR (CH_2Cl_2 , cm^{-1}): 2004 sh and 1988 vs.

Structure Analysis. An outline of the crystallographic and data collection parameters is given in Table I. Crystals were grown by allowing a solution of the complex in $\text{CH}_2\text{Cl}_2/\text{Et}_2\text{O}$ to stand for several days. Several air-stable, large, long needles were formed. A section of one of these was cut to size and mounted on the end of a glass fiber. Cell dimensions were based upon a Delaunay reduction of a cell obtained from the centering of 25 reflections on the diffractometer.

Intensity data (294 K) were measured with Mo $\text{K}\alpha$ radiation from a graphite monochromator (ω -2 θ scan, 96 steps/scan, 16 steps/side background). The intensities of three standard reflections were measured after each 7200-s exposure to the X-rays and showed no intensity decay during the experiment. No absorption correction was needed based on ψ scans. A total of 5392 reflections were measured and averaged ($R = 0.032$ on intensity) to give 4898 independent reflections. The Enraf-Nonius SDP program package was used for all calculations.

The structure was resolved by Patterson and Fourier methods. Hydrogen atoms were placed in calculated fixed positions. Full-matrix least-squares refinement minimizing $\sum w(|F_o| - |F_c|)^2$ converged to the R values given in Table I. No extinction correction was applied. The final difference Fourier had the nine largest peaks (0.45–1.60 e/Å³) in the vicinity of the CH_2Cl_2 molecule, indicating probable disorder. Final atomic positional parameters for the refined atoms are included in Table II. Selected bond distances and angles are given in Table III. Other data is included as supplementary material.

Acknowledgment. We thank the donors of the Petroleum Research Fund, administered by the American Chemical Society, the Research Corp., and the UMC Research Council for support of this work. A loan of RhCl_3 and IrCl_3 from Johnson Matthey is gratefully acknowledged. The National Science Foundation provided a portion of the funds for purchase of the X-ray (Grant CHE-7820347) and NMR (Grant PCM-8115599) equipment.

Supplementary Material Available: Tables of supplementary positional parameters (Table IIS), thermal parameters (Table SI), calculated hydrogen atom positional parameters (Table SII), torsion angles (Table SIII), dppm bond distances (Table SIV), dppm bond angles (Table SV), nonbonded distances to fluorine atoms (Table SVI), and least-squares planes (Table SVII) (16 pages); a listing of structure factors (42 pages). Ordering information is given on any current masthead page.

(18) Voge, H. H.; Adams, C. R. *Adv. Catal.* **1967**, *17*, 151.

(19) Barteau, M. A.; Madix, R. J. *J. Am. Chem. Soc.* **1983**, *105*, 344–349 and references cited therein.

(20) Hoffman, D. M.; Hoffmann, R. *Inorg. Chem.* **1981**, *20*, 3543–3555.

(21) (a) Fischer, G. B.; Gland, J. L. *Surf. Sci.* **1980**, *94*, 446–455. (b) Spitzer, A.; Luth, H. *Surf. Sci.* **1982**, *120*, 376–388.

(22) Burfield, D. R.; Lee, K.-H.; Smithers, R. H. *J. Org. Chem.* **1977**, *42*, 3060–3065.

(23) Supplementary material.